LAWRENCE
LIVERMORE
NATIONAL
LABORATORY

UCRL-PROC-222141

A Strategy for Interpretation of Microearthquake Tomography Results in the Salton Sea Geothermal Field Based upon Rock Physics Interpretations of State 2-14 Borehole Logs

Brian Bonner, Lawrence Hutchings, and Paul Kasameyer

June 16, 2006

Geothermal Resource Council Annual Meeting
September 10–13, 2006
San Diego, California

A Strategy for Interpretation of Microearthquake Tomography Results in the Salton Sea Geothermal Field Based upon Rock Physics Interpretation of State 2-14 Borehole Logs

Brian Bonner, Lawrence Hutchings, and Paul Kasameyer

Lawrence Livermore National Laboratory, P.O. Box 808, Livermore, CA 94551

Abstract

We devise a strategy for analysis of *Vp* and *V*s microearthquake tomography results in the Salton Sea geothermal field to identify important features of the geothermal reservoir. We first interpret rock properties in State 2-14 borehole based upon logged core through the reservoir. Then, we interpret seismic recordings in the well (Daley et al., 1988) to develop the strategy. We hypothesize that mapping Poisson's ratio has two applications for the Salton Sea geothermal reservoir: (1) to map the top of the reservoir, and (2) as a diagnostic for permeable zones. Poisson's ratio can be obtained from *Vp* and *V*s. In the State 2-14 borehole, Poisson's ratio calculated from large scale averages (~150 m) shows a monotonic decrease with depth to about 1300 m, at which point it increases with depth. Our model is that the monotonic decrease is due to compaction, and the increase below 1300 m is due to the rocks being hydrothermally altered. We hypothesize we can map the depth to alteration by identifying the transition from decreasing to increasing values; and thus, map the top of the reservoir, which is associated with a known increase in sulfite, chlorite, and epidote alteration that may be indicative of hydrothermal activity. We also observe (from Daley et. al. plots) an anomalous drop in Poisson's ratio at a depth of about 900 m, within a sandstone formation. The sandstone has a P-wave velocity significantly higher than the siltstone above it but a lower velocity in the lower half of the formation relative to the upper half. We interpret the relative decrease in velocity to be due to fracturing and chemical alteration caused by permeability. We conclude that using *Vp* and *V*s tomography results to obtain images of Poisson's ratio has the potential to identify significant features in the geothermal reservoir in this geologic setting. Seismic attenuation tomography results (mapped as *Qp* and *Qs*) should also be useful for evaluating geothermal reservoirs, but that is not addressed at this time.

Introduction

As part of a project to process and interpret more than ten years of surface seismic recordings of microearthquakes in the Salton Sea geothermal field, we devise a strategy for analyzing microearthquake tomography results to improve understanding of the geothermal reservoir. Seismic tomography uses signals from microearthquakes recorded by a surface network of seismometers to generate a three-dimensional distribution of seismic propagation properties. That approach has been used successfully in geothermal fields (Zucca et al., 1993; Ramero et al., 1997; Julian et al., 1999). The 3220-m-deep State 2-14 well was drilled at the edge of the Salton Sea geothermal field as part of the 1986 Salton Sea Scientific Drilling Project (SSSDP; Elders and Sass, 1988) (Figure 1). Changes in borehole conditions with depth of drilling and temperature limited the log suite available to depths less than 2000 m.

To develop a strategy for using tomography results, we use recordings from State 2-14 borehole (Daley et al., 1988) as an analog for the type of data we obtain from tomography studies. Daley et al. conducted several vertical seismic profiles (VSP) in the borehole. A three-component seismometer was lowered into the borehole to record signals produced by a source on the surface. We examined data collected when the source was very near the borehole, so that the

travel path is well known and the vertical propagation properties can be determined. *Vp* , *Vs* , Q_p, and Q_s estimates obtained from these recordings are virtually the same parameters that can be obtained in tomography studies based upon surface recordings. By examining the well-logged seismic parameters and comparing their interpretations to known rock properties, we can develop our strategy. We first use rock physics interpretations of logged core through the geothermal reservoir to identify rock properties. Then, we test whether interpretations of the seismic *Vp* and *Vs* are possible to help identify drilling targets for geothermal production-well drilling. We do not interpret *Qp* and *Qs* at this time. We conclude that Poisson's ratio provides the best diagnostic for important features in the Salton Sea geothermal field. Traditionally, seismologists have examined Vp/Vs ratios to interpret lithology in geothermal regimes. There is not a linear relation between Vp/Vs and Poisson's ratio. Therefore, the behavior of lithology is different for these two parameters. We decided to use Poisson's ratio because it is a more direct physical interpretation of physical behavior.

Figure 1. Study area, station locations, and State well 2-14. Green dots show the preliminary locations of earthquakes from a 2005, Mw=5.0 earthquake swarm. This mostly outlines the location of the geothermal activity, but it also extend to State 2-14 borehole. Stars indicate station locations that provide data for the three-dimensional tomography studies.

Lithology and Geology as a Function of Depth

The effects of increasing pressures with depth should result in increase of velocity with depth, as it is expected, where fewer thin cracks remain open as pressure increases (Tarif et al., 1988; Boitnott and Bonner,1994). In practice, closing of cracks with depth is often accomplished through chemical filling in addition to mechanical pressure and might more reasonably be termed crack filling. At the State 2-14 borehole, the extreme temperature gradient also complicates the analogy since temperature increases generally decrease velocities in opposition to the pressure effect (Tarif et al., 1988). Another significant difficulty is the superposition of other trends on the pattern of geothermal alteration. The combination of geophysical log data and core sample analysis provides insight into sediment properties and trends in alteration as a function of depth that would not be given by either analysis separately (Paillet and Morin, 1988). In the State 2-14 borehole, the profiles of physical properties obtained by the logs indicate several different effects (Paillet and Morin, 1988): (1) change of apparent physical properties with depth caused by changing in situ environment (increasing temperature, pore fluid pressure, and overburden stress), (2) increasing degree of geothermal alteration with depth, (3) changes in borehole conditions with depth, (4) decrease in number and types of logs and degradation of quality with increasingly hostile environment (at depth), and (5) possible systematic change in sediment properties related to systematic changes in source area and mechanism of deposition (Paillet and Morin, 1988). Numbers (1), (2), and (5) are equally applicable to interpreting seismic inversion results. Number (5) is referring to systematic differences in sediment deposits due to changes in the environment at the time of deposition, e.g., a change from siltstone to sandstone. In situ confining pressure and temperature can have substantial effects on geophysical properties (Paillet and Morin, 1988).

Elders and Sass (1988) and Paillet et al. (1988) describe the lithology and alteration from the surface to 3220-m depth. Muramoto and Elders (1984) identify four mineralogic zones in the Salton sediments: (1) unaltered montmorillonite zone, <100°–190°C; (2) illite zone, <190°–250°C; (3) chlorite zone, 240°–300°C; and (4) feldspar zone, <300°C. They indicate that the

primary factor determining geophysical log response in these zones is the transition in clay mineral properties.

Seismic Velocities. Near-offset VSP data provides a direct measurement of vertical travel times to each receiver depth, allowing interval velocities to be computed between receivers. Daley et al. (1988) picked first arrivals times of P and S waves and interval velocities were calculated. Signals were recorded at intervals of 30.5 m and 152 m, so these velocities represent averages over those segments. When calculating velocities, a straight ray path was assumed and used to correct the borehole depth for extra propagation distance due to the 91-m source offset. Figure 2 shows *Vp* and *Vs* from Daley et al. (1988) and laboratory values of *Vp* and *Vs* obtained from intact cores (Tarif et al., 1988). Note the velocity deficit that often occurs between core and field values because of in-situ fracturing. Core samples are often not recovered from fractured zones, and experimental methods require relatively sound samples to withstand the processing required to produce specimens of the proper dimension for testing. Majer et al. (1988) VSP to identify fractures at The Geysers.

Figure 2. (a) *Vp* and (b) *Vs* are plotted as a function of depth. Black curves show data from Daley et al. (1988). Red data points indicate laboratory values obtained from Tarif et al. (1988).

Preliminary Rock Physics Interpretation of State 2-14 Well Data. Our intent is to use relationships between rock elastic properties and porosity, permeability, and fluid content to help interpret seismic field observations. These relationships are obtained by laboratory investigations and theoretical analysis (rock physics). A classic example of the use of rock physics is to identify gas in petroleum reservoir rocks by interpreting “bright spots” in reflection seismograms. Laboratory measurements and the theory of wave propagation in saturated porous media Gassmann (1951) explains that these anomalous reflections originated from regions of low acoustic impedance caused by pockets of trapped gas. The predictions were verified by drilling. We choose to use Poisson’s ratio, the elastic parameter that is formed by dividing the longitudinal strain in an elastic deformation by the associated transverse strain, as a key to our analysis. For a perfectly elastic material, such as rubber, Poisson’s ratio = 0.5. Poisson’s ratio is a valuable tool because it can be calculated from the velocities alone and is therefore insensitive to density variations caused by lithology.

Poisson’s ratio: $\sigma = \dfrac{V_p^2 - 2V_s^2}{2(V_p^2 - V_s^2)}$.

There is not a linear relation between *Vp/Vs* and Poisson’s ratio as shown in Figure 3. Seismologists have traditionally used *Vp/Vs* and Poisson’s ratio interchangeably because over the range of values often observed in seismic data ($0.2<\sigma<0.3$) the relationship is essentially linear. At the Salton Sea the values range from 0.08 to 0.35, and the behavior of lithologhy is different for these two parameters over this range. Theory suggests that Poisson’s ratios tend to be steady based on rock microstructure (Berryman et al., 2002). Analysis of the elasticity of porous materials shows that different pore shapes produce characteristic values for Poisson’s ratio. For example, dry materials with spherical pores are predicted to have Poisson’s ratios of 0.2, independent of porosity, for low porosity.

Figure 3. Vp/Vs plotted versus Poisson’s ratio.

We examine a permeable zone between about 915 and 960 m. Paillet et al. (1986, p. 14) identified a loss of circulation during drilling at a depth near 960 m, presumably a zone of relatively high permeability. Daley identified a zone of high reflectors at 915-m depth, which he attributed to fractures. He corroborated this finding with studies of cores taken between 918 and 920.5 m, which were found to have fractures that are "presently open and permeable" in a matrix of "chloritized and epidotized crossbedded sandstone and shales" (McKibben and Andes, 1986). Given uncertainties in depth, we assume all three studies are talking about the same depth, which we attribute to the lower half of the sandstone formation discussed below. Table 1 lists different parameters obtained from above, through, and below the sandstone layer. The depth of each parameter may be slightly different. Depth shifts in geophysical logging studies are common because different degrees of cable stretch occur and different depth-measurement systems are used (Hearst and Nelson, 1985). We hypothesize that this permeable zone is evident in plots of Poisson's ratio.

Table 1. Well log summary.

Depth m (ft)	V_p (Daley)	V_s (Daley)	Poisson's ratio	Percent sandstone	V_p (Tarif)	V_s (Tarif)
762 (2500)	2.93	1.89	0.14**	20		
780	2.93	—		0		
792	3.36	—		10		
810	2.74	—		10		
822 (2700)	3.03	—		10		
841	3.02	—		10		
854	3.03	—	0.28§	10		
872	3.03	1.81	0.22**	15		
884 (2900)	3.03	—	0.26§	30		
902†	3.616	—	0.27§	25		
914†‡	3.79	—	0.28§	25	3.30 (911)	1.75
932†	3.79	—		50		
944* (3100)	3.37	—		60		
962*	3.37	—		70	3.70 (954)	1.83
973*	3.04	—		40		
994	3.04	2.048	0.08**	20		
1005 (3300)	3.37	2.069	0.19**	15		
1024	3.37	—	0.26§	10		
1036	4.34	—		5		
1054 (3460)	4.34	—		2	3.75 (1060)	2,16

‡ Depth of sample (919 m) from Lin and Daily (1988).
† Poisson's ratio anomaly.
§ 150 m averaged values.
** 30 m averaged values.

Figure 4 shows Poisson's ratio as a function of depth from Daley et al. (1988). The smooth variation and dramatic decrease in Poisson's ratio with depth from 600 to about 1220 m are striking features of the data. The Daley et al. data, subject to the caveat that shear velocity data are sparse, trend smoothly from 0.35 to 0.18 over this depth range. As the authors point out, 0.35

is typical for sedimentary rocks. We suggest that the systematic decrease is consistent with compaction and lithification of the deltaic sediments present in the 2-14 borehole above the zone of more severe alteration that begins at 1220 m. Below, we discuss the possibility of mapping the depth to top of the severe alteration zone (epidote alteration) by looking for changes in slope of the Poisson's ratio versus depth. Here, we interpret the notch in Daley's Poisson's ratio at 910 m (the first green bar in Figure 4) to be associated with the fractured portion of the sandstone and, thus, the permeable zone of the sedimentary layer. It stands out in a depth interval where compliant porosity is steadily being eliminated by compaction.

Our interpretation of Figure 4 is that increased fracturing is reducing both compressional and shear velocities (as generally accepted). Crack closure caused by increases in effective pressure tends to increase Poisson's ratio, as observed in laboratory-scale measurements (Bonner and Schock, 1981). Therefore, the opening of compliant features may decrease Poisson's ratio for the sedimentary rocks at the Salton Sea. This local fluctuation is evident because of the stable background, as evidenced by the monotonic increase in Poisson's ratio.

Figure 4. Poisson's ratio from Daley et al. (1988).

Table 1 lists Daley's and Tarif's velocity values along with percentage of sandstone estimates from Paillet et al. and estimates of Poisson's ratio at depths through the zone of permeability. There is a zone with a high percentage of sandstone from about 880 to 970 m. As Table 1 shows, the velocity increases dramatically as the sandstone is entered, but is relatively lower in the lower half of that zone. We hypothesize that the velocity drops in the lower half because of local fracturing, providing the permeability.

We suggest that the systematic decrease is consistent with compaction and lithification of the deltaic sediments present in the 2-14 borehole above the zone of more severe alteration that begins at 1220 m and that it is smoothly varying. Geochemical softening of the shear modulus (Boinott and Bonner, 1994) apparently does not play a significant role in this depth interval, since this effect would tend to increase Poisson's ratio. The stable background observation is supported by laboratory measurements made by Lin and Daily (1988). These authors determined compressional and shear velocities for a sample described as a siltstone with a porosity of 24.5%, recovered from 919 m (possibly in the permeable zone we are analyzing). The experimenters altered pressure and temperature to simulate in situ conditions for increasing depth on the rock matrix, providing the opportunity to isolate the effects of pressure and temperature on velocity. For a simulated depth range of 600 to 1220 m, Poisson's ratio trends downward in agreement with the field data, but at a much slower rate than is seen in data from State 2-14. The reduction in Poisson's ratio is estimated from the Lin and Daily measurements (their Figure 4b) as about 0.03, about 16% of the decrease observed by Daley et al.

Lin and Daily also compared their laboratory compressional velocity measurements with sonic log data. At depths shallower than the sample depth, laboratory velocities are faster than log velocities; below the sample depth, the sonic velocities are higher than those of the Lin and Daily sample at equivalent pressure and temperature conditions (Figure 5). At the temperature and pressure conditions seen in situ, the recovered core seems to retain velocity to within 10%, implying that its state of lithification is not altered greatly by coring. The more pronounced

changes in Poisson's ratio and sonic velocity observed in the field data do not arise from the combined effect of pressure and temperature, but appear to be associated with a steady increase in lithification and densification from geochemical alteration that stiffens the rock with increasing depth by systematically filling compliant, crack like features in preference to filling of rounded pores.

Poisson's ratio monotonically increases until about a depth of 1300 m, at which point it increases rapidly to about 0.25. Below this depth, Poisson's ratio stays fairly constant but has a higher variability than for shallower depths. We hypothesize we can map the depth to epidote alteration by identifying the transition from monotonic decrease to relatively constant values. This change in alteration is associated with the top of the reservoir. The increase in sulfite, chlorite, and epidote alteration noted in lithographic logs may be indicative of hydrothermal activity. The lithology remains fairly consistent from about 975 m to at least 1800 m, with primarily claystone (Paillet et al., 1986). Daley et al. also associate the rapid increase in Poisson's ratio with a known increase in sulfite, chlorite, and epidote alteration noted in lithographic logs that may be indicative of hydrothermal activity (Elders and Sass, 1986).

Figure 5. Ultrasonic P-wave travel time as a function of depth measured in the laboratory (points) and in situ from the borehole sonic log (lines). (From Lin and Daily, 1988.)

Conclusions

High-quality seismic data near State 2-14 well provide an opportunity to investigate the relationships between seismic velocities and the rock properties constrained by borehole data. Poisson's ratio may be a parameter that can be mapped in three dimensions from local microearthquake tomography to yield important information about geothermal reservoirs. By analyzing laboratory and field observations, we observed that: (1) localized volumes with relative decrease Poisson's ratio may indicate heavily fractured zones that might be permeable zones and 2) the vertical derivative of Poisson's ratio may indicate fractured zones where the dominant process is compaction / lithification of the original matrix of the rocks.

We hypothesize that mapping Poisson's ratio has two applications for the Salton Sea geothermal reservoir. It can be used (1) as a diagnostic for permeable zones and (2) to map the top of the reservoir. These conclusions are suggested by theoretical rock physics analysis and laboratory observations of rocks from the Salton Sea.

References

Berryman, J.G., P.A. Berge, and B.P. Bonner, 2002. "Estimating Rock Porosity and Fluid Saturation Using Only Seismic Velocities." *Geophysics*, v. 67, No. 2, p. 391–404.

Berge, Patricia, Lawrence Hutchings, Jeffrey Wagoner, and Paul Kasameyer (2001) Rock Physics Interpretation of P-wave Q and Velocity Structure, Geology, Fluids and Fractures at the Southeast Portion of The Geysers Geothermal Reservoir**.** Geothermal Res. Council, Transactions, 14, 2001 Annual Meeting, San Diego, CA.

Boitnott, G.N., and B.P. Bonner,1994. "Characterization of Rock for Constraining Reservoir Scale Tomography at the Geysers Geothermal Field." *Proceedings, Nineteenth Workshop on Geothermal Reservoir Engineering*. Stanford University, Stanford, CA, January 18–20, SGO-TR-147, p. 231-236.

Bonner, B.P. and R.N. Schock, 1981. Seismic Wave Velocity, Chapter 8, Physical Properties of Rocks and Minerals. McGraw-Hill/CINDAS Data Series on Material Properties, Vol. II-2.

Daley, T.M., T.V. McEvilly, and E.L. Majer, 1988. "Analysis of P and S Wave Vertical Seismic Profile Data from the Salton Sea Scientific Drilling Project." *J. Geophys. Res.* v. 93, No. B11, p. 13,025–13,036.

Elders, W.A., and J.H. Sass, 1988. "The Salton Sea Scientific Drilling Project. *J. Geophys. Res.* v. 93, No. B11, p. 12,953–12,968.

Gassmann, F., 1951. (translated, Berryman, "Origin of Gassmann's Equationis". Geophysics 64. 1627-1629, 1999.

Julian, Bruce R., Gillian Foulger, and Keith Richards-Dieger, 1999. The Coso Geothermal Area: A Laboratory for Advanced MEQ Studies for Geothermal Monitoring. Geothermic 42.

Hearst, J.R., and P.H. Nelson, 1985. *Well Logging for Physical Properties*. New York: McGraw-Hill, p. 571.

Lin, Wunan and William Daily, 1988. Laboratory-Determined Transport Properities of Core From the Salton Sea Scientific Drilling Project. *J. Geophys. Res.* v. 93, No. B11, p. 13,047–13,056.

Majer, E.L., T.V. McEvilly, F.S. Eastwood, L.R. Myer, 1988. Fracture Detection using P-wave and S-wave Vertical Seismic Profiling at The Geysers. Geophysics 63, 199.

McKibben, M.A., and J.P. Andes, 1986. "Ore Mineralization and Related Fluid Inclusion Properties in the SSSDP Cores." *Report to the SSSDP Principal Investigators' Session*. Geothermal Resources Council Meeting, Palm Springs, CA, September 1986.

Paillet, F.L., R.H. Morin, R.E. Hodges, L.C. Robison, S.S. Priest, J.H. Sass, J.D. Hendricks, P.W. Kasameyer, G.A. Pawloski, R.C. Carlson, A.G. Duba, J.R. Hearst, and R.L. Newmark, 1986. *Preliminary Report on Geophysical Well-Logging Activity on the Salton Sea Scientific Drilling Project, Imperial Valley, California*. U.S. Geological Survey, Open-File Report 86-544.

Paillet, F.L., and R.H. Morin, 1988. "Analysis of Geophysical Well Logs Obtained in the State 2-14 Borehole, Salton Sea Geothermal Area, California." *J. Geophys. Res.* v. 93, No. B11, p. 12,981–12,994.

Ramero Jr, A.E., T.V., and E.L. Majer, 1997. 3-D Microearthquake Attenuation Tomography at the Northwest Geysers Geothermal Region, California. Geophysics 62, 149.

Tarif, P.A., R.H. Wilkens, and C.H. Cheng, 1988. "Laboratory Studies of the Acoustic Properties of Samples From Salton Sea Scientific Drilling Project and Their Relation to Microstructure and Field Measurements." *J. Geophys. Res.* v. 93, No. B11, p. 13,057–13,067.

Zucca, J.J., L.J. Hutchings, and P.W. Kasameyer, 1994. Seismic Velocity and Attenuation Structure of the Geysers Geothermal Field, California. *Geothermics* **23**, 111-126.

Acknowledgments

This work was performed under the auspices of the U.S. Department of Energy by University of California, Lawrence Livermore National Laboratory under Contract W-7405-Eng-48.

Keywords: rock physics, tomography, geothermal, Poisson's ratio

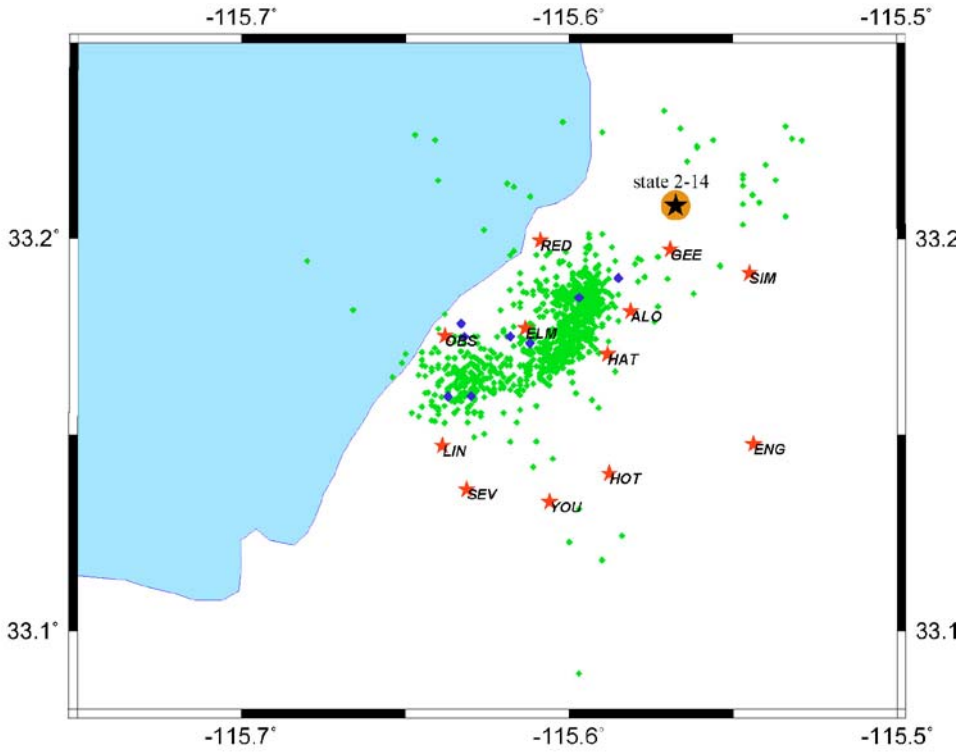

Figure 1. Study area, station locations, and State well 2-14. Green dots show the preliminary locations of earthquakes from a 2005, Mw=5.0 earthquake swarm. This mostly outlines the location of the geothermal activity, but it also extend to State 2-14 borehole. Stars indicate station locations that provide data for the three-dimensional tomography studies.

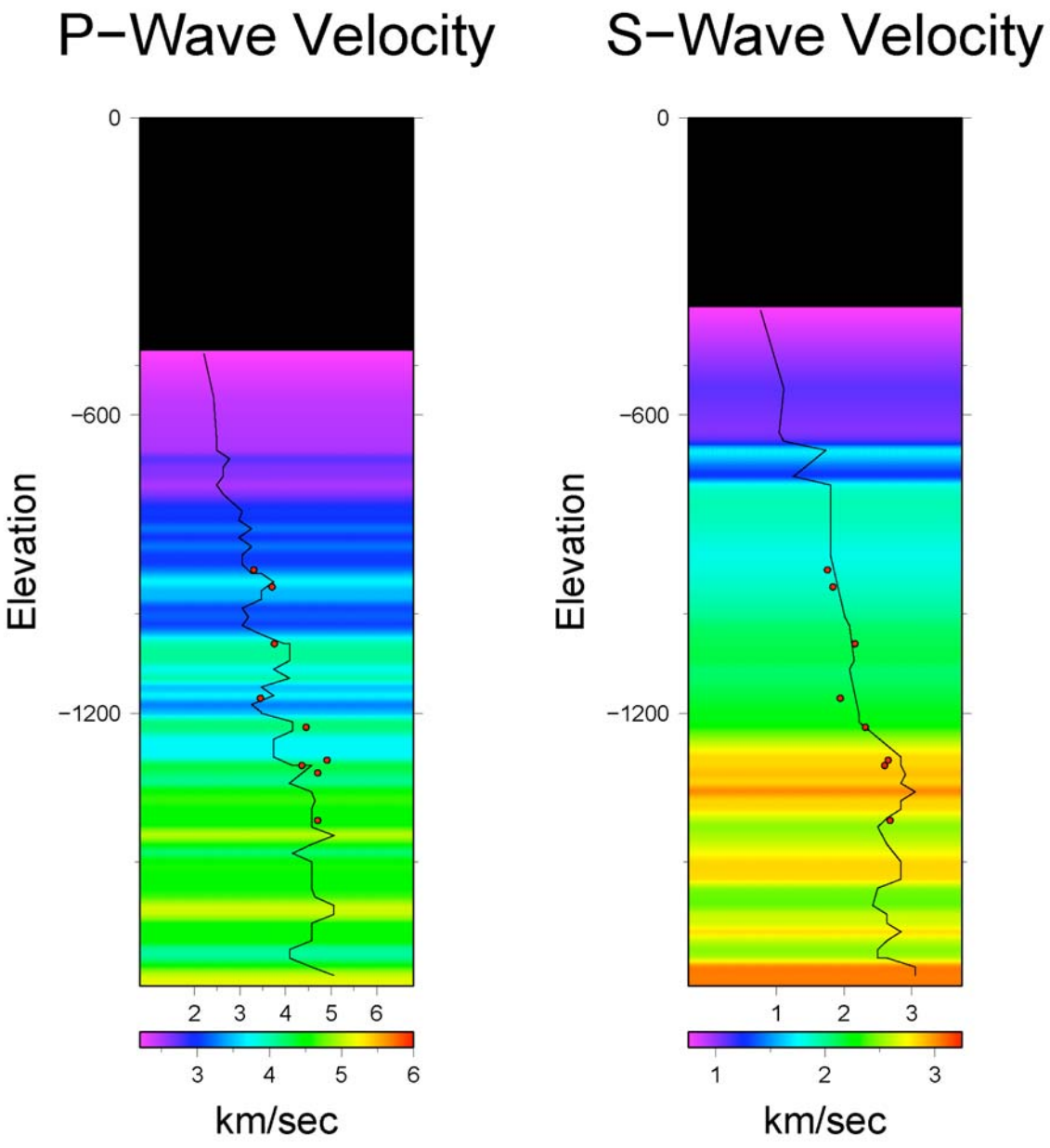

Figure 2. (a) *Vp* and (b) *Vs* are plotted as a function of depth. Black curves show data from Daley et al. (1988). Red data points indicate laboratory values obtained from Tarif et al. (1988).

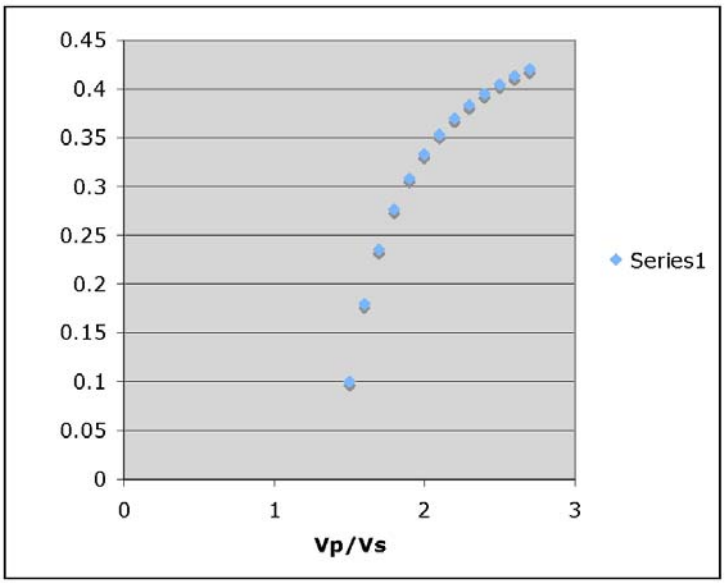

Figure 3. *Vp/Vs* plotted versus Poisson's ratio.

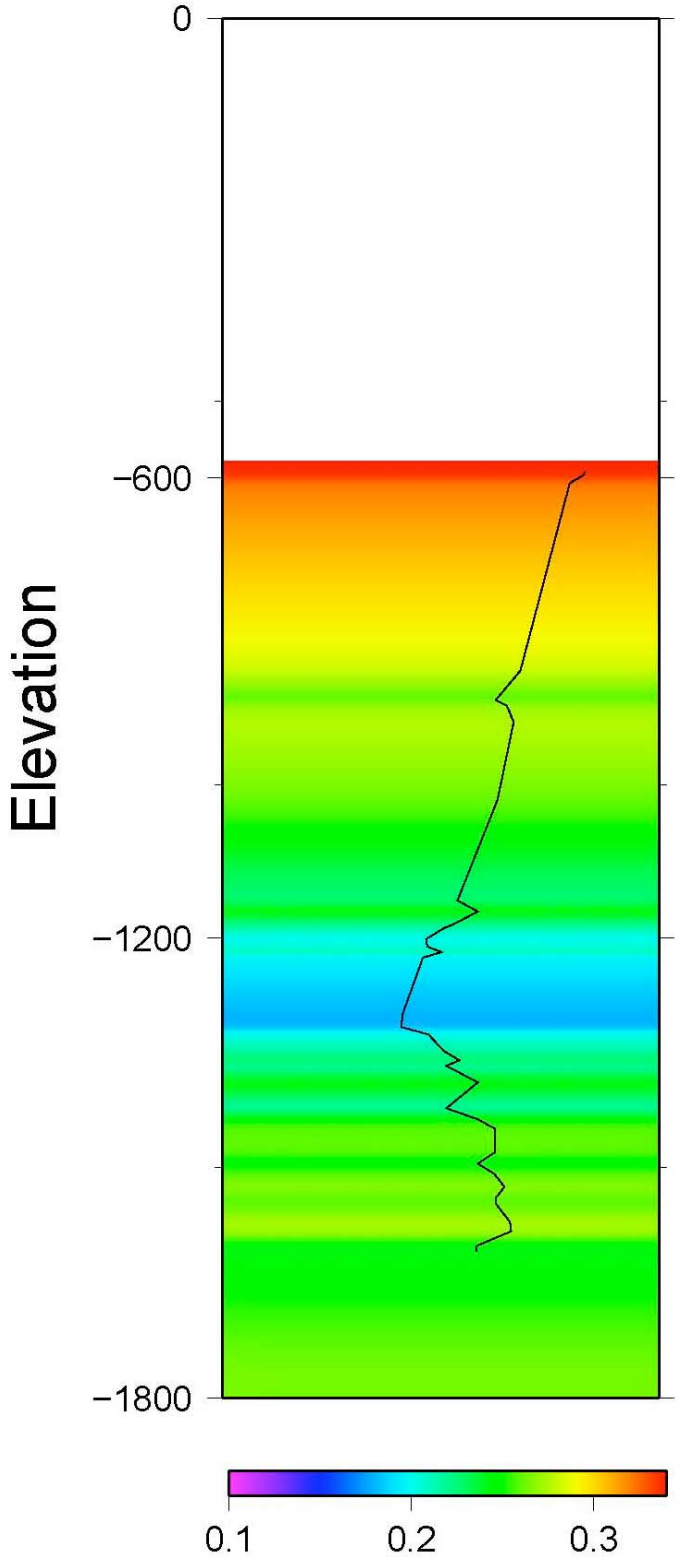

Figure 4. Poisson's ratio from Daley et al. (1988).

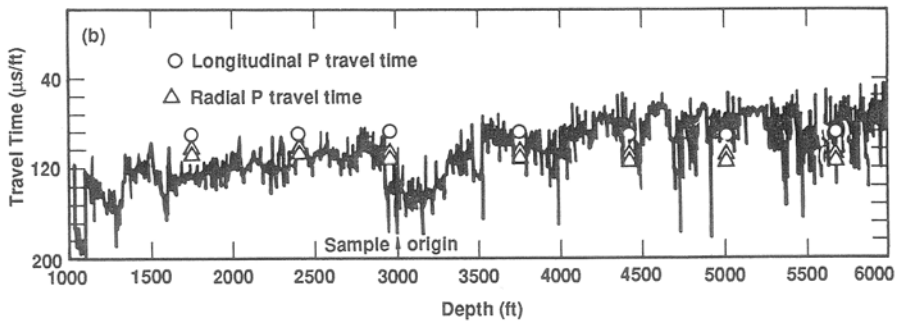

Figure 5. Ultrasonic P-wave travel time as a function of depth measured in the laboratory (points) and in situ from the borehole sonic log (lines). (From Lin and Daily, 1988.)